International Journal of Science and Research (IJSR)
ISSN (Online): 2319-7064
Index Copernicus Value (2015): 78.96 | Impact Factor (2015): 6.391

Yellow Luminescence from $LaAlO_3:Sm^{3+}$ Nano-Phosphors Prepared by Sol-Gel Technique

Subhash Chand[1], Ishwar Singh[2]

[1]Department of Chemistry, Maharshi Dayanand University, Rohtak-124001, Haryana, India

[2]PDM University, Sector 3A, Sarai Aurangabad, Bahadurgarh-124507, Haryana, India

Abstract: ***$LaAlO_3:Sm^{3+}$, nano-phosphors with varying dopant concentrations of Sm^{3+} from 1 to 20 mol% were prepared by Sol-Gel Synthesis and the samples were further heated to 600,700, and 1000 ^{0}C to improve the crystallinity of the materials. The advantages of gel combustion base process have been applied to obtain nano particles in the pure homogeneous form . Finally the phosphor was characterized by XRD, SEM, PL measurement to check the crystallinity, particles size and luminescence intensity of the phosphor respectively. XRD results reveal that the sample begins to crystallize at 600°C , and pure $LaAlO_3$ phase can be obtained at 700°C. SEM images indicate that the Sm^{3+} -doped LaAlO3 phosphors are composed of aggregated spherical particles with sizes ranging from 40 to 80nm . Under the excitation of UV light (245nm) and low-voltage electron beams (1–3kV), the Sm^{3+} -doped $LaAlO_3$ phosphors show the characteristic emissions of phosphor consist of five emission peaks, which are attributed to the transitions from $^4G_{5/2}$ state to ^6H_J (J=5/2, 7/2, 9/2, 11/2 ,13/2) states of Sm^{3+} ions with Yellow, Orangish-Yellow , Orangish-red and red color having emission peak located at 565, 598, 615, 653, 707 nm respectively . Among these emission peaks, the transition emission $^4G_{5/2}\rightarrow{}^6H_J$ (J=5/2, 7/2, 9/2) for peak at 565, 598, 615nm is strongest for Yellow, Orangish-Yellow and Orangish-red emission is due to the magnetic dipole transition of Sm^{3+} ion having a magnetic dipole (MD) allowed one and also an electric dipole (ED) dominated one but the other weak transition $^4G_{5/2}\rightarrow{}^6H_{11/2}$ & $^4G_{5/2}\rightarrow{}^6H_{13/2}$ (653 nm, 707nm red) is purely an ED one. Highest photoluminescence intensity is observed with 3 mol% doping of Sm^{3+} made $LaAlO_3:Sm^{3+}$, a strong competitor for promising Yellow, Yellow-orange & also for Orange-red colored display applications.***

Keywords: Sol-gel synthesis, Nano-phosphors, $LaAlO_3:Sm^{3+}$, Host lattices, Co-dopants , Magnetic dipole, Electric dipole.

1. Introduction

Presently the development of flat panel displays, such as field emission displays (FEDs), plasma display panels (PDPs) and thin film electro-luminescent devices (TFEL), or white light emitting diode (LED), have emerged as the principal motivation for research into rare-earth luminescence, and the present article therefore concentrates on the variety of different ways in which rare-earth luminescence has been exploited in this field[1–4] . The rare-earth ions are characterized by a partially filled 4f shell that is well shielded by $5s^2$ and $5p^6$ orbitals. The emission transitions, therefore, yield sharp lines in the optical spectra. The use of rare-earth element based phosphor, based on "line-type" f–f transitions,[5-7] can narrow to the visible, resulting in both high efficiency and a high lumen equivalent [8]. It is, therefore, urgent to find a stable, inorganic rare-earth-based phosphor with high luminescent efficiency. The phases composed by the elements with the smaller difference of electronegativity (X), corresponds to a narrower band gap of compounds, leading to higher conductivity. The difference between the electronegativities of Si and O (X= 1.54) exceeds that between Ge and O (X= 1.43)[9]. During the past decades, rare earth ions doped in various host materials have been widely studied due to their characteristic luminescence properties. Among the rare earth ions,Sm^{3+} ,Eu^{3+} , Tb^{3+} , and Dy^{3+} are important activator ions for producing visible light [10–17]. Sm^{3+} activated luminescent materials have received much attention at present [18-19]. They show bright emissions in orange and red regions attributed to the transitions from the excited state $^4G_{5/2}$ to the ground state $^6H_{5/2}$ and the other state ^6H_J (J = 7/2, 9/2 , and 11/2), which can be used in high density optical storage, temperature sensors, under sea communication, various fluorescent devices, color display, and visible solid-state lasers [20–21]. Luminescence of is especially useful to probe the local structure of luminescent centers in a host lattice because of its simple energy level structure, great sensitivity to ligand field, and similar lanthanide chemical properties to the other rare earth ions [22-23]. Growing interest recently has been focused on luminescence of trivalent rare earth ions in phosphates, tungstates, borates, molybdates, and aluminates, among which rare earth doped borates are especially attractive because of their wide UV transparency, exceptional optical damage thresholds, excellent chemical and thermal stability, and high luminescence efficiency[24–34]. The luminescence study of a series of such compounds provides much valuable information for optical applications.

It is our main interest to synthesize another family of newly developed Sm^{3+} doped phosphors via low temperature initiated gel based combustion process and investigate their photoluminescence properties in view of the commercial importance of yellow and orangish-red color emitting phosphors. Generally, the typical Sm-activated phosphors usually show charge-transfer absorption of Sm^{3+} $–O^{2–}$ interaction in the UV region. However, there was no obvious charge-transfer absorption of $Sm^{3+}– O^{2–}$ interaction or host absorption band that could be detected in the excitation spectrum. Only direct excitation of Sm^{3+} ions could be observed. It is recognized that Sm^{3+} interaction with the host lattice is very weak, and no energy transfer occurs between Sm^{3+} and host. As we know different material preparation methods such as solid state reactions, sol-gel techniques[35], hydroxide precipitation[36], hydrothermal synthesis[37], spray pyrolysis[38], laser evaporation[39] and combustion

synthesis [40- 42] has been investigated for the preparation of oxide phosphors. These methods have their advantages as well as limitations. In multi step processes like heating at high temperatures and long processing time are required. The sol-gel method is a novel technique through which a voluminous, foamy nano crystalline powder can be prepared within a few minutes. This technique is ideal for producing the fine, pure and single-phase powders. have some important effects on material microstructure and physical properties. The sol-gel method provides an interesting alternative over other elaborated techniques because it offers several attractive advantages such as: simplicity of experimental set-up; surprisingly short time between the preparation of reactants and the availability of the final product; and being cheap due to energy saving.

The main aim of the sol-gel is the rapid decomposition of the rare earth nitrate in the presence of an organic fuel. During the reaction, many gases, such as CO_2, N_2, NO_2 [43] and H_2O, as well as a large amount of heat are released in a short period of time before the process terminates with white, foamy and crispy products. Many times final products are found to be composed of nano-sized particles. This work has been carried out with the aim to prepare ,compare and investigate the high intensity photoluminescence nano sized crystalline powders of $LaAlO_3$ doped with Sm^{3+} sintered at 1000ºC temperature.

A series of $La_{1-x}Sm_xAlO_3$ phosphor have been synthesized by sol-gel method with the dopant concentration ranging from 01 to 20 mol%. The crystalline structure and morphology of prepared nano-materials have also been discussed. The crystalline structure of prepared materials, morphology of particles and their photoluminescence properties are characterized by XRD, SEM and PL spectra with 245 nm lasers for excitation. The present work is mainly focused on preparation characterization & discussion on the $LaAlO_3$:Sm^{3+} nano phosphor showing high luminescence.

2. Experimental

All the chemicals used were of high purity (Aldrich 99.99%). High purity chemicals $La(NO_3)_3$, $Al(NO_3)_3$, $Sm(NO_3)_3$, in such a way that total [La^{3+} + Sm^{3+}] = 1.0 mole, and carbohydrazide as a fuel were used to prepare Sm^{3+} doped nano crystals with general formula $La_{(1-x)}AlO_3$: Sm_x^{3+} , where x is 1 to 20 mol%. This mixture was heated in a crucible on a hot plate for about half an hour to form a viscous gel. After evaporating most of the water contents, crucible was placed into a microwave oven for 5 minutes to propagate for the combustion reaction which is done in a preheated furnace maintained at 600,700, and 1000 ^{0}C to improve the crystallinity of the materials. XRD results reveal that the sample begins to crystallize at 600°, and pure $LaAlO_3$ phase can be obtained at 700°C. The stoichiometric amount of the fuel was calculated by using total oxidizing and reducing valences [43]. The paste was made by dissolving metal nitrates and fuel in a minimum amount of doubly distilled water. In furnace, the material had rapid dehydration followed by decomposition, generating combustible gases which burnt with a flame and producing a white solid. The solid thus obtained was again fired at 1000°C for 3h to increase the crystallinity. Finally the powder was characterized by XRD, SEM, PL measurement to check the crystallinity, particles size and luminescence intensity of the phosphor respectively.

3. Characterization & Discussion

3.1 XRD studies

The structural characterizations of compounds were done on XRD diffractometer (Rigaku Ultima IV) using Cu Kα radiation (1.541841 Å).

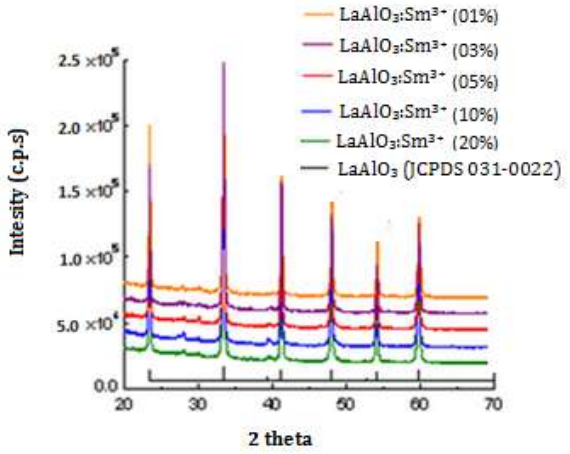

Figure1: XRD spectra of $LaAlO_3$:Sm^{3+} phosphors showing sharp xrd peaks.

The structural characterizations of compounds were done on XRD diffractometer (Rigaku Ultima IV) using Cu Kα radiation**.** XRD results reveal that the sample begins to crystallize at 600°C , and pure $LaAlO_3$ phase can be obtained at 700°C . Crystallinity, particle size, and surface roughness of the phosphor materials have strong effects on the photoluminescence. Fig1. showed the X-ray diffractograms of Sm^{3+} doped $LaAlO_3$ $LaAlO_3$:Sm^{3+} phosphors . The phase analysis demonstrated (Fig.1) that $LaAlO_3$:Sm^{3+} belongs to trigonal crystal system with R3m (160) space group having unit cell dimensions: a =b = 5.364 Å and c = 13.11 Å. This was in good agreement with the standard JCPDS C. NO. 031-0022. In this phosphor, trivalent lanthanum ions were replaced by trivalent samarium ions. Dopant ions (Sm^{3+}) concentration variation from 1mol % to 10 mol% have no noticeable effect on the obtained X-ray diffractograms of the as-prepared $LaAlO_3$:Sm^{3+} phosphors, indicating that the doped ions were occupied the primordial La^{3+} sites of the $LaAlO_3$ lattice**.** All measurements were carried out at room temperature. The structural characterization was done by a high resolution X-ray diffraction (XRD) using a Rigaku Ultima IV diffractometer in the θ–2θ configuration and using Cu Kα radiation (1.5418 Å) using Scherrer equation (1).

$$\tau = K\lambda / \beta \cos\theta \qquad (1)$$

where

- τ is the mean size of the ordered (crystalline) domains, which may be smaller or equal to the grain size;

- K is a dimensionless shape factor, with a value close to unity. The shape factor has a typical value of about 0.9, but varies with the actual shape of the crystallite;
- λ is the X-ray wavelength;
- β is the line broadening at half the maximum intensity (FWHM), after subtracting the instrumental line broadening, in radians. This quantity is sometimes denoted as (2θ);
- θ is the Bragg angle was used to calculate the crystallite size of all materials.

At least five prominent peaks from each XRD (samples with various Sm^{3+} concentration) were used for calculation and peaks belonging to different phases were also taken into consideration. Maximum and minimum values obtained for each type of lattice are reported as range of crystallite size (e.g. 40±5nm for $LaAlO_3$).

3.2 SEM micrograph and particle size analysis

The SEM micrographs were obtained by JEOL JSM6300 scanning electron microscope. SEM images indicate that the Sm^{3+} - doped $LaAlO_3$ phosphors are composed of aggregated spherical particles with sizes ranging from 40±5 nm.

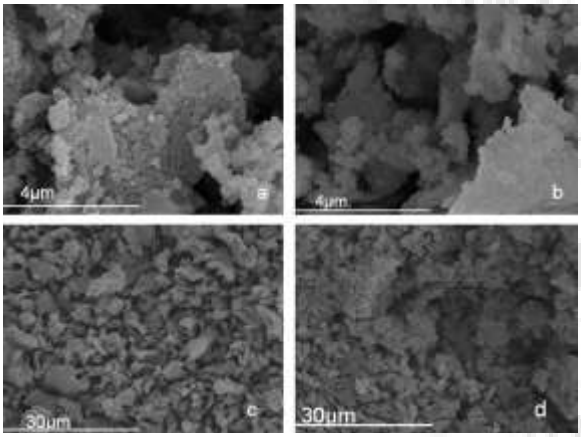

Figure2: SEM micrographs of phosphor particles (a,b, c, d,): (a) $LaAlO_3$ lattice (b to d) $LaAlO_3:Sm^{3+}$

Figures 2 (a to d) exhibited the surface morphologies of $LaAlO_3$, $LaAlO_3:Sm^{3+}$ particles. Generally non-uniformity of shape and size is associated with the non-uniform distribution of temperature and mass flow in the combustion flame. However the SEM images of $LaAlO_2:Sm^{3+}$ particles (fig. 2a,b) show small and coagulated particles of nearly cubical shape with larger size distribution. The surface morphology of $LaAlO_2:Sm^{3+}$ lattices as depicted in the picture 2a and 2b is smooth and aggregated spherical particles of different sizes are observed. The smooth surface of phosphor can reduce the non-radiation and scattering, thus beneficial to the luminescence efficiency in application[44-45]. The dence packed small particles can prevent the phosphor from aging.

3.3 Photoluminescence Properties

For the photoluminescence measurement, 0.05g powder samples were pressed into pellets and then exposed to a He–Cd laser (245nm) with an optical power of 30mW for excitation. The emitted light was analyzed by HR-4000 Ocean Optics USB spectrometer optimized for the UV–vis range. Under the excitation of UV light (245nm) and low-voltage electron beams (1–3kV) , the Sm^{3+} -doped LaAlO3 phosphors show the characteristic emissions of the Sm^{3+} at $^4G_{5/2}\rightarrow{}^6H_J$ (J=5/2 , 7/2 , 9/2, 11/2 , 13/2) transitions and strongest yellow, Yellow-orange & Orange-red color with $^4G_{5/2}\rightarrow{}^6H_J$ (J=5/2 , 7/2 , 9/2) . The room-temperature emission spectra of Sm^{3+} doped $LaAlO_3$ crystals with different doping concentrations are shown in figures 3 (a to b). The emission spectra were obtained by monitoring at 245nm under an excitation of ultraviolet light. The obtained products emitted the red luminescence of varying intensities, which showed the activator Sm^{3+} had successfully entered the host lattice of $LaAlO_3$. The characteristic emissions of phosphor consist of five emission peaks, which are attributed to the transitions from $^4G_{5/2}$ state to ^6H_J (J=5/2, 7/2, 9/2, 11/2,13/2) states of Sm^{3+} ions . Among these, emission peak located at 565-577, 598, 617-619, 653-655, 708-709, are attributed to the transitions of $^4G_{5/2}\rightarrow{}^6H_{5/2}$, $^4G_{5/2}\rightarrow{}^6H_{7/2}$, $^4G_{5/2}\rightarrow{}^6H_{9/2}$, $^4G_{5/2}\rightarrow{}^6H_{11/2}$ and $^4G_{5/2}\rightarrow{}^6H_{13/2}$, respectively [44-50]. Among these emission peaks, the transition emission $^4G_{5/2}\rightarrow{}^6H_{7/2}$ (565nm, strongest yellow, a strong Yellow-orange located at 598nm & 615 nm for orange-red color due to the $^4G_{5/2}\rightarrow{}^6H_{J=5/2\ ,\ 7/2\ ,\ 9/2}$ magnetic dipole transition of Sm^{3+} ion having a magnetic dipole (MD) allowed one and also a electric dipole (ED) dominated one and the other transition $^4G_{5/2}\rightarrow{}^6H_{J=11/2\ ,13/2}$ (653 nm, 708-709nm, red) is purely an ED one. The MD transition does not appreciably depend on the chemical surroundings of the luminescent center and its symmetry; however, the ED transition belongs to hypersensitive transitions. Generally, the intensity ratio of ED to MD transitions has been used to evaluate the symmetry of the local environment of the trivalent 4f ions. The greater the intensity of the ED transition, the more the asymmetry nature [51]. The exact positions of emission peaks in various lattices are shown in table 1. The $^4G_{5/2}\rightarrow{}^6H_{J=5/2\ ,\ 7/2\ ,\ 9/2}$ transition is well known to be mainly a magnetic dipole transition when the Sm^{3+} ions locate in a high symmetric position while the $^4G_{5/2}\rightarrow{}^6H_{J=11/2\ ,13/2}$ transitions are essentially electric dipole transitions which appear only when Sm^{3+} ion locates at sites without inversion symmetry [52-53]. In fig 3, the emission intensity of all peaks increased with increase of doping concentration from 1% to 3 mol % and then starts decreasing. It becomes nearly one fifth with 20 mol% doping of Sm^{3+} in $LaAlO_3:Sm^{3+}$ phosphors. The emission and decay behaviors of the $^4G_{5/2}\rightarrow{}^6H_{7/2}$ transition depend on the concentration of Sm^{3+} ions. The emission intensity increases with Sm^{3+} concentration up to 3 mol%, and then decreases quickly. The decay time also begins to decrease rapidly at around 3 mol%. At higher concentrations (x> 0.03), however, the observed decay were non-exponential, and the non-exponential change becomes more prominent as (Sm^{3+}) content increases, revealing that more than one relaxation process exists. It is expected that with the increase of Sm^{3+} ions, photoluminescence should increase. However, the emission intensity tends to decrease above 3 mol% of Sm^{3+} ions due to concentration quenching [54], because of non-radiative interaction between ions as the resonant energy transfer becomes stronger. As the concentration is increased, the Sm^{3+} ions are packed closer and closer together, which favors the transfer of energy from

one Samarium ion to the next by a resonance process; the energy eventually reaches a sink from which it is dissipated by non-radiative processes rather than by the emission of visible light [55-56].

Table 1: The emission peaks in $LaAlO_3:Sm^{3+}$ nano-phosphors

Lattice	$^4G_{5/2}\rightarrow{}^6H_{5/2}$ Yellow (nm) Strong peak	$^4G_{5/2}\rightarrow{}^6H_{7/2}$ & $^4G_{5/2}\rightarrow{}^6H_{9/2}$ Yellowish - - Orange & Orangish — -Red (nm) Strong	$^4G_{5/2}\rightarrow{}^6H_{11/2}$ & $^4G_{5/2}\rightarrow{}^6H_{13/2}$ Red (nm) Weak peak
$La_{0.99-0.097}Sm_{0.01-0.03}AlO_3$	565	598,614,625	655 655,708
$La_{0.95}Sm_{0.05}AlO_3$	577	598 & 615	653 & 709
$La_{0.90}Sm_{0.10}AlO_3$	565	599 ,612,625	654, 708
$La_{0.80}Sm_{0.20}AlO_3$	575	598,612,	654,708

In the present case, the emission spectrum shows three strong sharp peaks at the 565, 598nm and 615nm corresponding to the magnetic dipole transition ($^4G_{5/2}\rightarrow{}^6H_{J=5/2\ ,\ 7/2\ ,\ 9/2}$) and electric dipole transition ($^4G_{5/2}\rightarrow{}^6H_{J=5/2\ ,\ 7/2\ ,\ 9/2}$) of Sm^{3+} emission respectively. Other weak intensity peaks are seen on right side of these three strong peaks. It may be mentioned that similar results from magnetic dipole transition ($^4G_{5/2}\rightarrow{}^6H_{J=5/2\ ,\ 7/2\ ,\ 9/2}$) were observed for Sm^{3+} doped $LaAlO_3$ host [57] and the strong yellow, yellow-orange & orange-red emission of the prepared $LaAlO_3:Sm^{3+}$ nano-phosphors had already not been proposed for its probable utility for display applications.

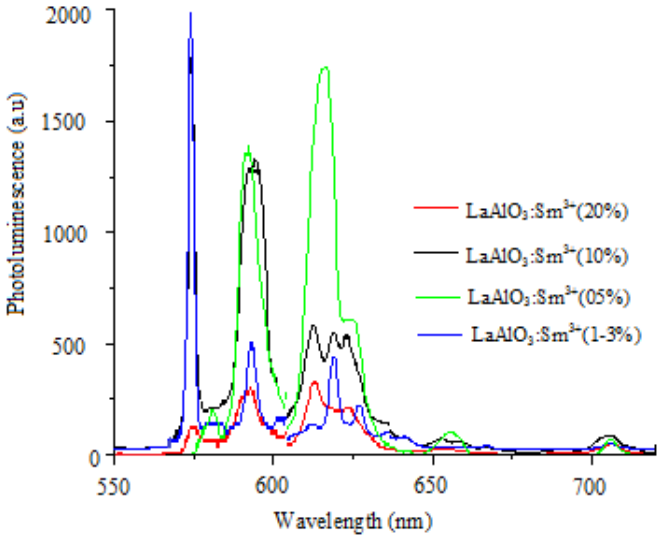

Figure 3: PL spectra of $LaAlO_3:Sm^{3+}$ phosphors showing yellow, yellow –orange & orange-red emission.

Earlier workers observed these peaks only in the Sm^{3+} doped $LaAlO_3$ host which substantiate the presence of Sm^{3+} ions [57-58]. The intensity ratio of 598 nm peak to 615 nm peak is a measure of asymmetry of the Sm^{3+} site in the host lattice [59]. Luminescence study shows that magnetic dipole transition ($^4G_{5/2}\rightarrow{}^6H_{J=5/2\ ,\ 7/2\ ,\ 9/2}$) is prominent over the other electric dipole transition ($^4G_{5/2}\rightarrow{}^6H_{J=11/2\ \ 13/2}$), which is attributed to occupancy of inversion symmetry site by more Sm^{3+} ions in Sm^{3+} doped $LaAlO_3$. If more Sm^{3+} ions have occupancy at the inversion site, the emission intensity from the ($^4G_{5/2}\rightarrow{}^6H_{J=5/2\ ,\ 7/2\ ,\ 9/2}$) transition will enhance and the phosphor will primarily exhibit orange luminescence. In the present investigation, the intensity of ($^4G_{5/2}\rightarrow{}^6H_{J=5/2\ ,\ 7/2\ ,\ 9/2}$) transition is comparable to the intensity of other electric dipole transition ($^4G_{5/2}\rightarrow{}^6H_{J=11/2\ ,\ 13/2}$).

4. Conclusion

$LaAlO_3:Sm^{3+}$, nano-phosphors with varying dopant concentrations of Sm^{3+} from 1 to 20 mol% were prepared by sol-gel synthesis and the samples were further heated to 600,700, and 1000 ^{0}C to improve the crystallinity of the materials. The advantages of gel combustion base process have been applied to obtain nano particles in the pure homogeneous form. Finally the phosphor was characterized by XRD, SEM, PL measurement to check the crystallinity, particles size and luminescence intensity of the phosphor respectively. XRD results reveal that the sample begins to crystallize at 600°C , and pure $LaAlO_3$ phase can be obtained at 700°C. SEM images indicate that the Sm^{3+} -doped LaAlO3 phosphors are composed of aggregated spherical particles with sizes ranging from 40 to 80nm. Under the excitation of UV light (245nm) and low-voltage electron beams (1–3kV), the Sm^{3+} -doped $LaAlO_3$ phosphors show the characteristic emissions of phosphor consist of five emission peaks, which are attributed to the transitions from $^4G_{5/2}$ state to ^6H_J (J=5/2, 7/2, 9/2, 11/2 ,13/2) states of Sm^{3+} ions with Yellow, Orangish-Yellow , Orangish-red and red color having emission peak located at 562, 598, 615, 653, 707 nm respectively . Among these emission peaks, the transition emission $^4G_{5/2}\rightarrow{}^6H_J$ (J=5/2, 7/2, 9/2) for peak at 562, 598, 615nm is strongest for Yellow, Orangish-Yellow and Orangish-red emission is due to the magnetic dipole transition of Sm^{3+} ion having a magnetic dipole (MD) allowed one and also an electric dipole (ED) dominated one but the other weak transition $^4G_{5/2}\rightarrow{}^6H_{11/2}$ & $^4G_{5/2}\rightarrow{}^6H_{13/2}$ (653 nm, 707nm red) is purely an ED one. Highest photoluminescence intensity is observed with 3 mol% doping of Sm^{3+} made $LaAlO_3:Sm^{3+}$, a strong competitor for promising Yellow, Yellow-orange & also for Orange-red colored display applications. The prepared $LaAlO_3:Sm^{3+}$ nano-phosphors had already been proposed for its probable utility for display applications and so became more attractive for further research work.

5. Acknowledgments

This nano-phosphor had been prepared in Inorganic Lab no 218, Deptt. of Chemistry , M.D.U Rohtak-124001, Haryana, India. by Dr. Subhash Chand Chopra, under supervision of Senior Professor Ishwar Singh, Pro-Vice Chancellor, P.D.M University , Bahadurgarh-124507, Haryana, India. & with support of Professor V.K. Sharma, H.O.D Chemistry, Department of Chemistry, M.D.U Rohtak.

References

[1] C. Duan, J. Yuan, X. Yang, J. Zhao, Y. Fu, G. Zhang, Z. Qi, Z. Shi, J. Phys. D: Appl. Phys. 38 (2005) 3576.
[2] A. Komeno, K. Uematsu, K. Toda, M. Sato, J. Alloys Compd. 408–412 (2006) 871.
[3] A.H. Kitai, Thin Solid Films 445 (2003) 367.
[4] V. Sivakumar, U.V. Vardaraju, J. Electrochem. Soc. 152 (10) (2005) H168.
[5] O. V. Solovyev, and B. Z. Malkin,"Modeling of electron-vibrational $4f^n$–$4f^{n-1}5d$ spectra in $LiYF_4:RE^{3+}$ crystals," Journal of Molecular Structure, 838, pp. 176-181, 2007.
[6] K. Ogasawara, S. Watanabe, H. Toyoshima, M.G. Brik, "Handbook on Physics and Chemistry of Earths", **37**, pp.1-59, 2007.
[7] C. Shi, J. Shi, J. Deng, Z. Han, Y. Zhou, G. Zhang, *J. Electron Spectrosc. Phenom.*, **79**, 121,1996
[8] C. Feldmann, T. Justel, C.R. Ronda, P.J. Schmidt, Adv. Funct. Matter 13 (7) (2003) 511.
[9] J.E. Hubeey, Inorganic Chemistry: Principles of Structure and Reactivity, 2nd ed., Harper and Row Publisher Inc., New York, 1978.
[10] N. S. Hussain, G. Hungerford, R. El-Mallawany et al., "Absorption and emission analysis of RE3+(Sm3+ and Dy3+): Lithium boro tellurite glasses," Journal of Nanoscience and Nanotechnology, vol. 9, no. 6, pp. 3672–3677, 2009.
[11] M. D. Que, Z. P. Ci, Y. H. Wang, G. Zhu, Y. R. Shi, and S. Y. Xin, "Synthesis and luminescent properties of Ca2La8(GeO4)6O2:RE3+ (RE3+=Sm3+, Tb3+, Dy3+, Sm3+, Tm3+) phosphors," Journal of Luminescence, vol. 144, pp. 64–68, 2013.
[12] A. Tang, D. F. Zhang, and L. Yang, "Photoluminescence characterization of a novel red-emitting phosphor In2(MoO4)3:Sm3+ for white light emitting diodes," Journal of Luminescence, vol. 132, no. 6, pp. 1489–1492, 2012.
[13] S. A. Naidu, S. Boudin, U. V. Varadaraju, and B. Raveau, "Sm3+ and Tb3+ emission in molybdenophosphate Na2Y(MoO4)(PO4)," Journal of the Electrochemical Society, vol. 159, no. 4, pp. J122–J126, 2012. View at Publisher ·
[14] X. L. Dong, J. H. Zhang, X. Zhang, Z. D. Hao, and S. Z. Lv, "Synthesis and photoluminescence properties of Sm2+ doped Sr9Sc(PO4)7 phosphors for white light-emitting diodes," Ceramics International, vol. 40, no. 4, pp. 5421–5423, 2014.
[15] P. Abdul Azeem, M. Kalidasan, R. R. Reddy, and K. Ramagopal, "Spectroscopic investigations on Tb3 doped lead fluoroborate glasses," Optics Communications, vol. 285, no. 18, pp. 3787–3791, 2012.
[16] E. Cavalli, P. Boutinaud, R. Mahiou, M. Bettinelli, and P. Dorenbos, "Luminescence dynamics in Tb3+-doped CaWO4 and CaMoO4 crystals," Inorganic Chemistry, vol. 49, no. 11, pp. 4916–4921, 2010.
[17] A. Boukhris, M. Hidouri, B. GloriSmx, and M. Ben Amara, "Correlation between structure and photoluminescence of the Smropium doped glaserite-type phosphate Na2SrMg(PO4)2," Materials Chemistry and Physics, vol. 137, no. 1, pp. 26–33, 2012.
[18] Y. Zhang, C. H. Lu, L. Y. Sun, Z. Z. Xu, and Y. R. Ni, "Influence of Sm2O3 on the crystallization and luminescence properties of boroaluminosilicate glasses," Materials Research Bulletin, vol. 44, pp. 179–183, 2009.
[19] M. Sobczyk, P. Starynowicz, R. Lisiecki, and W. Ryba-Romanowski, "Synthesis, optical spectra and radiative properties of Sm2O3:PbO:P2O5 glass materials," Optical Materials, vol. 30, no. 10, pp. 1571–1575, 2008.
[20] V. Venkatramu, P. Babu, C. K. Jayasankar, T. Tröster, W. Sievers, and G. Wortmann, "Optical spectroscopy of Sm3+ ions in phosphate and fluorophosphate glasses," Optical Materials, vol. 29, no. 11, pp. 1429–1439, 2007.
[21] S. Nishiura, S. Tanabe, K. Fujioka, and Y. Fujimoto, "Properties of transparent Ce:YAG ceramic phosphors for white LED," Optical Materials, vol. 33, no. 5, pp. 688–691, 2011.
[22] X. M. Zhang and H. J. Seo, "Luminescence properties of novel Sm3+, Dy3+ doped LaMoBO6 phosphors," Journal of Alloys and Compounds, vol. 509, pp. 2007–2010, 2011.
[23] A. M. Pires, M. F. Santos, M. R. Davolos, and E. B. Stucchi, "The effect of Sm3+ ion doping concentration in Gd2O3 fine spherical particles," Journal of Alloys and Compounds, vol. 344, no. 1-2, pp. 276–279, 2002.
[24] K. Driesen, V. K. Tikhomirov, and C. Gorller-Walrand, "Sm3+ as a probe for rare-earth dopant site structure in nano-glass-ceramics," Journal of Applied Physics, vol. 102, Article ID 024312, 2007.
[25] C. H. Yan, L. D. Sun, C. S. Liao et al., "Sm3+ ion as fluorescent probe for detecting the surface effect in nanocrystals," Applied Physics Letters, vol. 82, no. 20, pp. 3511–3513, 2003.
[26] R. Stefani, A. D. Maia, E. E. S. Teotonio, M. A. F. Monteiro, M. C. F. C. Felinto, and H. F. Brito, "Photoluminescent behavior of SrB4O7:RE2+ (RE=Sm and Sm) prepared by Pechini, combustion and ceramic methods," Journal of Solid State Chemistry, vol. 179, no. 4, pp. 1086–1092, 2006.
[27] Y. Won, H. Jang, W. Im, D. Jeon, and J. Lee, "Red-emitting LiLa2O2BO3: Sm3+, Sm3+ phosphor for near-ultraviolet light-emitting diodes-based solid-state lighting," Journal of The Electrochemical Society, vol. 155, no. 9, pp. J226–J229, 2008.
[28] M. Ayvacıklı, A. Ege, and N. Can, "Radioluminescence of SrAl2O 4:Ln3+ (Ln = Sm, Sm, Dy) phosphor ceramic," Optical Materials, vol. 34, no. 1, pp. 138–142, 2011.
[29] Y. M. Yang, Z. Y. Ren, Y. C. Tao, Y. M. Cui, and H. Yang, "Sm3+ emission in SrAl2B2O7 based phosphors," Current Applied Physics, vol. 9, pp. 615–621, 2009.
[30] D. Tu, Y. J. Liang, R. Liu, Z. Cheng, F. Yang, and W. L. Yang, "Photoluminescent properties of LiSrxBa1−xPO4:RE3+ (RE = Sm3+, Sm3+) f–f transition phosphors," Journal of Alloys and Compounds, vol. 509, no. 18, pp. 5596–5599, 2011.
[31] J. H. Hao, J. Gao, and M. Cocivera, "Tuning of the blue emission from Smropium-doped alkaline earth chloroborate thin films activated in air," Applied Physics Letters, vol. 82, no. 17, pp. 2778–2780, 2003.
[32] A. E. Henkes and R. E. Schaak, "Synthesis of nanocrystalline REBO3 (RE=Y, Nd, Sm, Sm, Gd, Ho) and YBO3:Sm using a borohydride-based solution

precursor route," Journal of Solid State Chemistry, vol. 181, no. 12, pp. 3264–3268, 2008.
[33] G. F. Ju, Y. H. Hu, H. Y. Wu et al., "A red-emitting heavy doped phosphor Li6Y(BO3)3:Sm3+ for white light-emitting diodes," Optical Materials, vol. 33, pp. 1297–1301, 2011.
[34] J. Yang, C. M. Zhang, C. X. Li, Y. G. Yu, and J. Lin, "Energy transfer and tunable luminescence properties of Sm3+ in TbBO3 microspheres via a facile hydrothermal process," Inorganic Chemistry, vol. 47, no. 16, pp. 7262–7270, 2008.
[35] C.N. Rao, *Mater. Sci. Engg. B,* **1993**, 18, 1.
[36] K. M. Kinsman, J. Mckittrick, E. Sluzky, K. Hesse, *J. Am. Ceram. Soc.*, **1994**, 77 (11), 2866.
[37] C. D. Vietch, *J. Mater. Sci.*, **1991**, 26, 6527.
[38] Y.C. Kang, H.S. Roh, S. B. Park, *Adv. Mater*., **2000**, 12, 451.
[39] D. K. Wilams, B. Bhihari, B.M. Tissue, *J. Phys. Chem*., **1998**, B 102, 916.
[40] Y. Tao, G. W. Zhao, W.P. Zhang, S.D. Xia, *Mater. Res. Bull.*, **1997**, 32, 501.
[41] L.D. Sun, J. Yao, C.H. Liu, C.S. Liao, C.H. Yan, *J. Lumin.*, **2000**, 87-89, 447.
[42] T. Takeda, D. Koshiba, S. Kikkawa, *J. Alloy. Comp*., **2006**, 408-412, 879.
[43] S. Ekambaram, K. Patil, *J. Alloys Compd*., **248,** 7,1997.
[44] Y. Conga, B. Lia, B. Leia, X. Wanga, C. Liua, J. Liua, W. Li, J Lumin, 128, 2008, 105.
[45] G. Liu, G. Hong, J. Wang, X. Dong, *J. Alloys Compd*., **432**, 200, 2007.
[46] F. He, P. Yang, D. Wang et al., "Hydrothermal synthesis, dimension evolution and luminescence properties of tetragonal LaVO4:Ln (Ln = Sm3+, Dy3+, Sm3+) nanocrystals," Dalton Transactions, vol. 40, no. 41, pp. 11023–11030, 2011.
[47] G. S. R. Raju, J. Y. Park, H. C. Jung et al., "Excitation induced efficient luminescent properties of nanocrystalline Tb3+/Sm3+:Ca2Gd8Si6O26 phosphors," Journal of Materials Chemistry, vol. 21, no. 17, pp. 6136–6139, 2011.
[48] X. Lin, X. S. Qiao, and X. P. Fan, "Synthesis and luminescence properties of a novel red SrMoO4:Sm3+,R+phosphor," Solid State Sciences, vol. 13, no. 3, pp. 579–583, 2011.
[49] Z. Yang, Z. Zhao, M. Que, and Y. Wang, "Photoluminescence and thermal stability of β-SiAlON:Re (Re = Sm, Dy) phosphors," Optical Materials, vol. 35, no. 7, pp. 1348–1351, 2013.
[50] M. Puchalska and E. Zych, "The effect of charge compensation by means of Na+ ions on the luminescence behavior of Sm3+-doped CaAl4O7 phosphor," Journal of Luminescence, vol. 132, no. 3, pp. 826–831, 2012.
[51] G. Lakshminarayana, R. Yang, J. R. Qiu, M. G. Brik, G. A. Kumar, and I. V. Kityk, "White light emission from Sm3+/Tb3+ codoped oxyfluoride aluminosilicate glasses under UV light excitation," Journal of Physics D: Applied Physics, vol. 42, no. 1, , 2009.
[52] R. Ningthoujam, V. Sudarsan, S. Kulshreshtha, *J. Lumin*., **127** , 747,2007.
[53] X. Gao, L. Lei, C. Lv, Y. Sun, H. Zheng, Y. Cui., *J. Solid* State Chem., **181**, p.1776, 2008.
[54] F.S. Kao, *Mater. Chem. Phys.*, **2002**, 76, 295.
[55] E. Perea, M. Estrada, M. Gracia, *J. Phys.*, **31** , 7,1998.
[56] T. Hayakawa, N. Kamt, K. Yamada, *J. Luminesc*., **68**, 179, 1996.
[57] P. Deren, J. Krupa, *J. Lumin.*,2003, **102**, 386.
[58] D. Hreniak, W. Strek, P. Dereń, A. Bednarkiewicz,Łukowiak, *J. Alloys Compd.*, 2006, **408 ,** 828.
[59] G. Blasse, B. Grambier, *Luminescent Materials, Springer-Verlag*, 1994, p.43.

Author Profile

Dr. Subhash Chand Chopra, is a senior research scholar in the Department of Chemistry, M. D. University Rohtak-124001, Haryana, India and working on nano-material synthesis since 2008. Dr. Subhash Chand had published seven research paper in International Journal indexed with Thomson Reuter. He presented four research paper in national conference and four research paper in international conference. He attended two national workshop.